Latest and Greatest
in
Permanent Source/Seed Implantation (PSI)

Tarun K. Podder, PhD
Professor
Department of Radiation Oncology
Department of Biomedical Engineering
University Hospitals, Seidman Cancer Center
Case Western Reserve University
Cleveland, OH 44106

July 12, 2020

Learning Objectives (3rd/Final Talk)

1) Understand the importance of application of multimodal imaging in PSI

2) Learn the new and advanced methodologies and technologies available for PSI

Multimodal Imaging: detection & diagnosis

- US imaging has been the primary modality for prostate biopsy followed by pathological findings/diagnosis

- mpMRI (T2w, DWI, DCE, MRS) has become more and more popular over the last decades for the diagnosis of prostate cancer due to anatomical and functional imaging ability

- T2w MRI is mainly used for prostate boundary detection while the diffusion-weighted imaging is the modality choice for computer-aided prostate cancer detection

Can we avoid invasive biopsy and rely on digital biopsy?

| T1w MRI | T2w MRI | DWI MRI | DCE MRI |
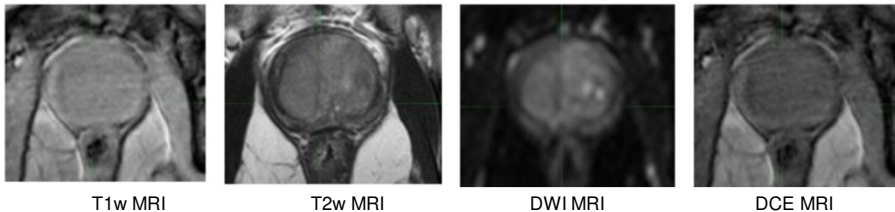
Multimodal Imaging: detection & diagnosis

mpMRI-based radiomics and AI/ML for cancer detection

AI – artificial intelligence
ML – machine learning
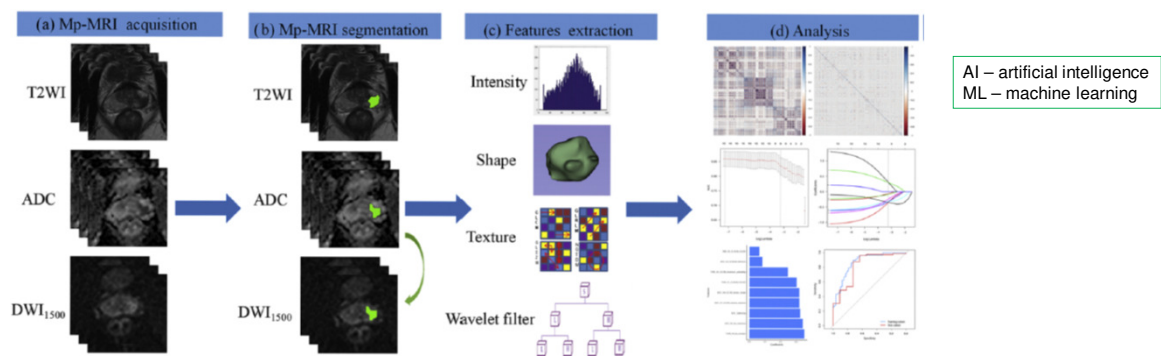
The framework for the radiomics workflow

(a) Patient scanned with preoperative mpMRI

(b) The dominate tumor was delineated by stacking up regions of interest slice-by-slice on the ADC map and transverse T2w image on each slice. The segmented volume of interest was copied from ADC maps to DWI_{1500} images

(c) High-throughput radiomics features were extracted from mpMRI

(d) Data analysis for feature selection, radiomics signature construction and testing

Multimodal Imaging: detection & diagnosis

mpMRI-based radiomics for cancer detection
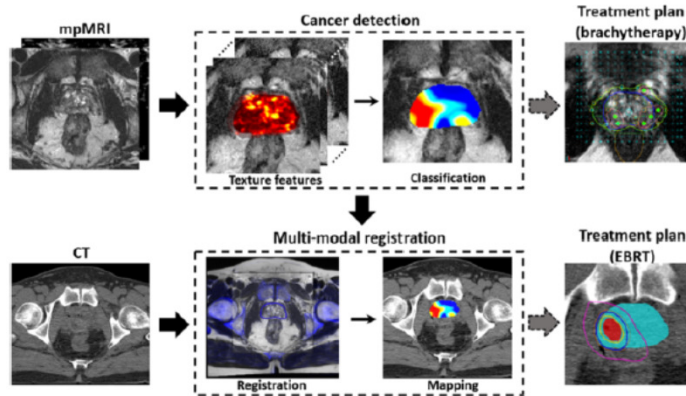
- An overview of the presented framework for radiomics assisted targeted treatment radiotherapy planning (Rad-TRaP) of prostate cancer

- Rad-TRaP consists of three modules - 1) voxel-wise cancer detection on MRI based on radiomic feature analysis, 2) transference of cancer delineations to CT via deformable registration of MRI and CT, and 3) generation of targeted focal radiotherapy plans for brachytherapy and EBRT
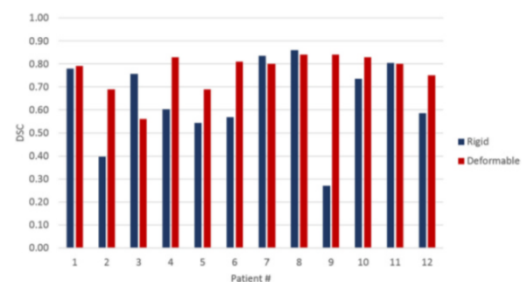
Shiradkar, Podder et al, Radiation Oncology (2016) 11:148

Multimodal Imaging: detection & diagnosis

mpMRI-based radiomics for cancer detection
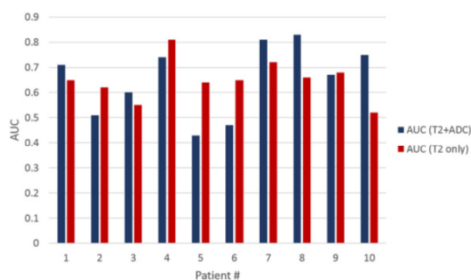
- Quantitative results of the voxel-wise predictions using the radiomics trained machine learning classifier in terms of AUCs for individual patients

- The classifier was trained on T2w, ADC MRI sequences and T2w alone to show that misalignment between T2w and ADC MRI affects the performance of the classifier (patients 2, 5 and 6)

- Dice similarity coefficients (DSC) evaluating the co-registration of T2w MRI and CT

- The DSCs from deformable registration are typically higher than those from rigid registration

Shiradkar, Podder et al, Radiation Oncology (2016) 11:148

3

Multimodal Imaging: detection & diagnosis

Deep convolutional neural networks (D-CNN) have been applied successfully for the diagnosis of cancers in general, and promising results have been achieved for prostate cancer.
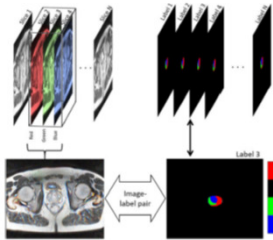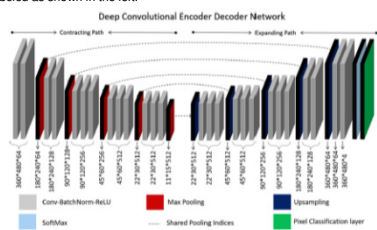

Illustration of sliding a 3D window across the input volume. Note that the label of the middle slice is considered as the label for the 3D window. In the dataset each pixel at each slice is labeled as shown in the left.

The architecture of the deep convolutional encoder-decoder network and used to segment lesions in MRI. Note that the dimensions under each layer corresponds to the size of the output activations produced by same layer.
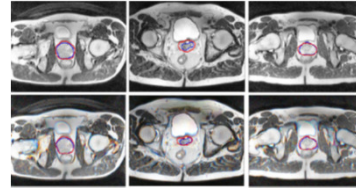

Prostate segmentation results of M1 and M2. The first row shows examples of segmentation performed using M1. The corresponding segmentation of M2 on the same slices is shown in the second row. The blue contour shows the ground truth segmentation, while the red contour shows the segmentation obtained by the proposed D-CNN algorithms.
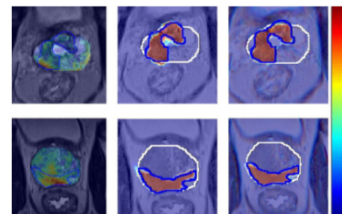
Results of prostate cancer detection produced by Lemaitre et al., M1 and M2 from left to right, respectively. White contour shows the prostate boundary segmented by a radiologist, while blue contour is the ground truth of malignant lesions. Note that each row shows the same slice and each column shows the performance of the same CAD system.

Alkadi, Taher et al, J of Digital Imaging (2019) 32:793–807

Multimodal Imaging: seed implant
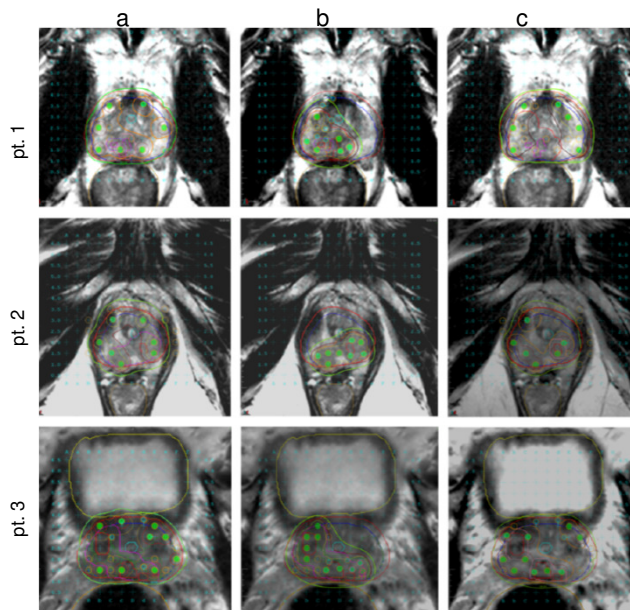
DIL (mpMRI vol.) - dominant intraprostatic lesion

Aim is to cover DIL/mpMRI volume with 150% of Rx dose

- Different treatment plans for brachytherapy shown on a single slice of T2w MRI for 3 different patients in 3 rows
  - **a** - whole gland (WH)
  - **b** - ref/focal area (RF)
  - **c** - whole gland + focal (WF)

- Plans in WH and WF cover the entire prostate (*blue contour*) and have a larger dosage (maroon colored contour shows V_{150})

- Number of needles (*green circles*) compared to RF in which only the cancerous region (*bright red contour* within the prostate) is covered

Shiradkar, Podder et al, Radiation Oncology (2016) 11:148

Dose painting to DIL or mpMRI Vol.

Pre-Operative and Post-operative dosimetric coverage of DIL volume with ^{125}I and ^{103}Pd

Parameter	Pre-Operative			Post-Operative		
	^{125}I	^{103}Pd	p-value	^{125}I	^{103}Pd	p-value
DIL V$_{100\%}$ (% vol)	99.8±2.9	99.9±0.2	0.83	99.8±0.6	99.2±2.5	0.89
DIL V$_{150\%}$ (% vol)	96.0±10.6	97.2±4.4	0.88	84.5±18.7	82.1±16.5	0.82
DIL V$_{200\%}$ (% vol)	63.8±17.3	72.1±13.5	0.05	51.0±24.1	51.8±23.2	0.13
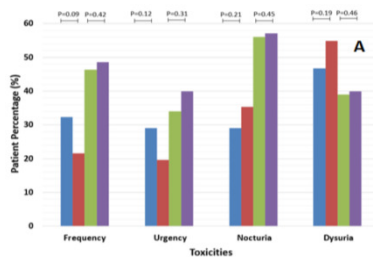
(A) - Incidence of urinary toxicities for patients with and without DIL treated with ^{125}I and ^{103}Pd.

DIL (mpMRI vol.) - dominant intraprostatic lesion

Aim is to cover DIL/mpMRI volume with 150% of Rx dose

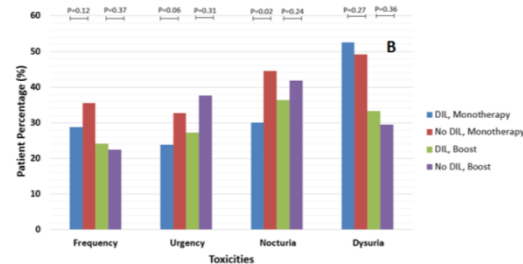(B) - Incidence of urinary toxicities for patients with and without DIL treated with PSI as monotherapy and boost.

Muenkel, Traughber et al, J Oncol Res (2019) 3(1): 01-14

Dose painting to DIL or mpMRI Vol.

Dosimetric parameters by group.

|	LDR only		LDR + Boost		p value
Disease characteristics	n	% (Range)	n	% (Range)	
Stage (NCCN)					
T1c	61	56	28	51	
T2a	16	15	13	24	0,226
T2b	28	26	14	26	
T2c	5	5	0	0	
Gleason's score					
6	57	52	28	51	
7 (3 + 4)	48	44	27	49	0,359
7 (4 + 3)	4	4	0	0	
Initial PSA level					
Median	6,3	(3,2-10,1)	6,1	(4,1-11,0)	
<10	81	74	38	69	0,424
≥10	29	26	17	31	0,583
Positive biopsy ratio (%)	21	(14-38)	28	(17-33)	0,333
Maximal invasion biopsy ratio (%)	20	(10-45)	20	(10-40)	0,461
Cytoreductive hormotherapy	8	7	12	22	0,011
Median	2,5	(1,5-3,0)	3,0	(3,0-6,0)	0,101

NCCN = National Comprehensive Cancer Network, PSA = Prostate-Specific Antigen, Range = First Quartile and Third Quartile

Genitourinary toxicities by group according to CTCAE v.4.03.

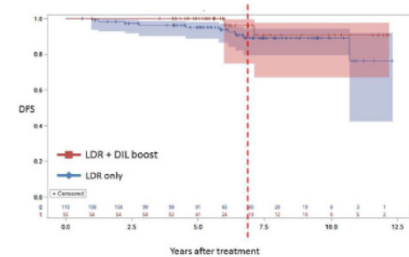| Toxicity	Grade	LDR only	LDR + Boost	P values
Acute (%)	1	58,1	51,9	0,118
	2	33,3	46,2	
	≥3	0	0	
Late (%)	1	50,5	60,4	0,076
	2	36,6	37,7	
	≥3	0	0,2	
Catheterism (n)		3	2	1,00

CTCAE = Common Terminology Criteria for Adverse Events.

DIL (mpMRI vol.) → dominant intraprostatic lesion;   Boost → boost to DIL
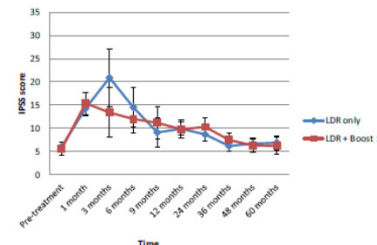
Mean IPSS score during follow-up by group
IPSS = International Prostate Symptom Score

Seven-year biochemical failure-free survival (7-year BFFS) curve.

Guimond, Lavallee et al., Radiotherapy and Oncology (2019) 133:62–67

Multimodal Imaging: dosimetric planning

Segmentation/ contouring – TRUS, CT, MRI

1) TRUS –
   - suitable for real-time, no radiation, inexpensive
   - low-contrast between the prostate and surrounding tissues, and the inter-exam variability of the prostate characteristics, inherent artifacts (speckle, shadowing, and attenuation)

2) CT – prostate contouring is challenging

3) MRI - good contrast compared to the TRUS and CT

Auto segmentation on MRI is based on automatically extracted features; used methods are CNN, deep learning for feature extraction.

Multimodal Imaging - promising results have been obtained by incorporating information of prostate gland shape from MRI with US or with CT.

Multimodal Imaging: dosimetric planning

1) Pre-Op planning – TRUS, CT, MRI
   - Determine seeds, order seeds, assay/verification (TRUS, CT, MRI)
   - Pre-loaded needles (TRUS)

2) Intra-Op planning – TRUS, real-time dosimetry

3) Post-Op planning – CT, MRI or a combination
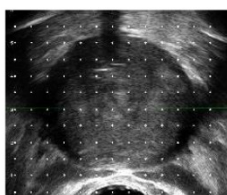
US image of prostate with LDR brachytherapy template grid on it.

CT image of prostate prior to EBRT and LDR implant.

Post LDR CT image of prostate. Seeds are seen as bright white spots.

** Accurate contouring of prostate on CT is very challenging

Brachytherapy Dose Computation

1) 1D/2D geometric formulation (TG-43)
2) Model based computation (TG-186)
3) Dosimetric evaluation (TG-137)

1-D dosimetry formulation (AAPM TG-43U1)

$$\dot{D}(r) = S_K \cdot \Lambda \cdot \frac{G_L(r,\theta_0)}{G_L(r_0,\theta_0)} \cdot g_L(r) \cdot \phi_{an}(r)$$

$\dot{D}(r)$ = dose rate to water at point $P(r)$
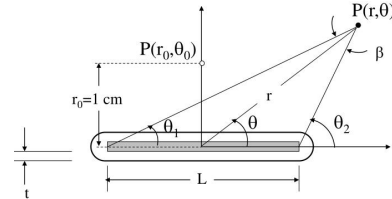S_K = air kerma strength
Λ = dose rate constant
$G_L(r,\theta)$ = geometric function (line source approximation)
$g_L(r)$ = radial dose function
$\phi_{an}(r)$ = 1-D anisotropy function

2-D dosimetry formulation (AAPM TG-43U1)

$$\dot{D}(r,\theta) = S_K \cdot \Lambda \cdot \frac{G_L(r,\theta_0)}{G_L(r_0,\theta_0)} \cdot g_L(r) \cdot F(r,\theta)$$

$\dot{D}(r,\theta)$ = dose rate to water at point $P(r)$
S_K = air kerma strength
Λ = dose rate constant
$G_L(r,\theta)$ = geometric function (line source approximation)
$g_L(r)$ = radial dose function
$F(r,\theta)$ = 2-D anisotropy function

Factor-based vs Model-based

	INPUT	CALCULATION	OUTPUT
TG43	Source characterization	Superposition of data from source characterization	$D_{\text{w-TG43}}$

	INPUT	CALCULATION	OUTPUT
MBDC	Source characterization / Tissue/applicator information	Model-Based Dose Calculation Algorithms	$D_{m,m}$ $D_{w,m}$
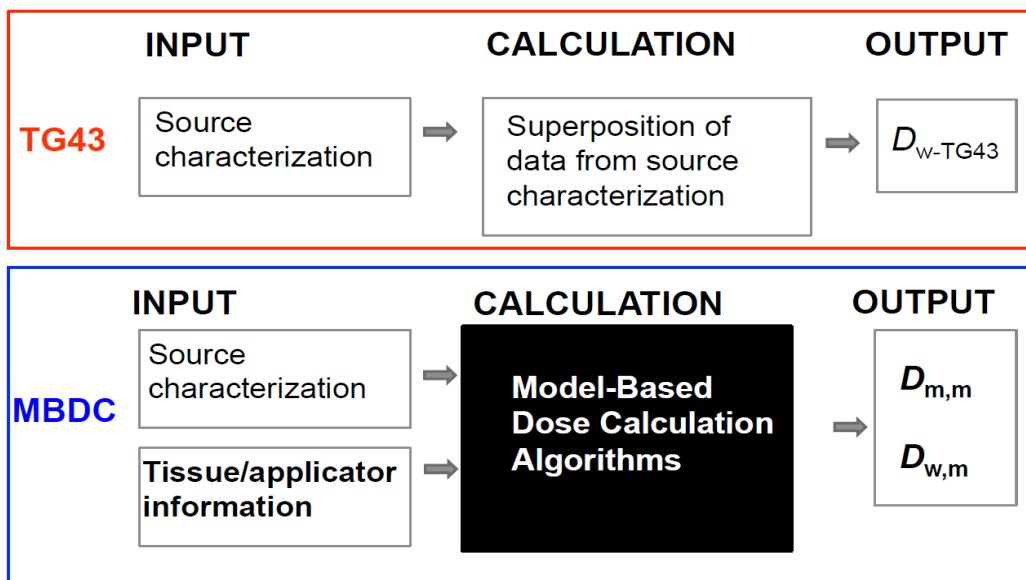
Brachytherapy Dose Computation (MBDC vs. TG43)

Dose metrics evaluated with **MCref/MBDC** and **TG43sim/TG43** for 613 patients and 3 example cases

	Target				Urethra			Rectum			Bladder		
	D_{90} (Gy)	D_{99} (Gy)	V_{100} (%)	V_{200} (%)	D_5 (Gy)	D_{30} (Gy)	V_{100} (%)	$D_{0.1cm3}$ (Gy)	D_{2cm3} (Gy)	D_{30} (Gy)	$D_{0.1cm3}$ (Gy)	D_5 (Gy)	D_{30} (Gy)
Overall results from 613 patients													
MCref	144.1	94.6	88.2	30.0	271.4	222.2	83.4	176.3	97.5	42.8	221.8	120.1	54.9
TG43sim	152.6	101.3	90.4	33.4	283.4	232.8	86.0	185.6	102.8	44.2	219.2	119.7	56.0
$\%\Delta_{av}$	−5.9	−7.2	−2.6	−11.5	−4.4	−4.7	−5.7	−5.2	−5.4	−3.2	1.3	0.4	−2.1
$\%\Delta_{std}$	1.6	2.5	1.7	3.2	1.8	1.9	6.5	1.8	1.7	5.3	1.8	1.5	2.0
IQR(MCref)	34.9	32.2	9.8	14.7	93.2	56.6	19.8	73.6	34.8	16.7	99.8	38.6	22.0
IQR(TG43sim)	36.6	33.8	9.2	16.9	97.5	58.6	17.7	76.0	36.8	18.4	98.9	38.5	22.1
Example case 1: 1.52 cm³ calcification													
MCref	110.4	72.4	73.3	19.7	230.8	182.6	79.1	121.4	64.6	25.1	224.6	97.9	34.9
TG43sim	137.4	98.4	87.6	22.7	267.3	223.8	93.2	152.5	81.8	31.8	229.2	99.7	38.7
$\%\Delta$	−24.4	−35.9	−19.4	−15.5	−15.8	−22.6	−17.8	−25.6	−26.6	−26.6	−2.1	−1.8	−10.9
Example case 2: 0.32 cm³ calcification													
MCref	84.9	54.5	61.7	13.6	190.3	168.7	59.8	86.9	54.4	21.7	86.2	45.2	19.3
TG43sim	92.9	60.5	68.4	15.2	203.7	183.3	68.4	94.1	58.6	23.5	87.0	44.4	20.6
$\%\Delta$	−9.5	−11.0	−10.8	−12.1	−7.1	−8.6	−14.4	−8.3	−7.6	−8.5	−0.9	1.9	−7.0
Example case 3: no CT visible calcification													
MCref	114.2	73.5	79.1	20.5	193.6	162.0	59.0	99.4	62.4	27.2	247.0	141.1	70.4
TG43sim	120.9	78.4	82.0	22.6	201.2	167.3	62.0	105.0	66.7	29.5	254.6	141.3	71.9
$\%\Delta$	−5.9	−6.8	−3.6	−10.1	−4.0	−3.3	−5.2	−5.6	−6.9	−8.4	−3.1	−0.1	−2.1

MCref: CT-derived heterogeneous tissue model with interseed effects

Miksys, Vigneauly et al., IJROBP (2019) 97(3):606-615

Sensitivity of Anatomic Sites to Dosimetric Limitations of Current Planning Systems

anatomic site	photon energy	absorbed dose	attenuation	shielding	scattering	beta/kerma dose
prostate	high					
	low	XXX	XXX	XXX		
breast	high				XXX	
	low	XXX	XXX	XXX		
GYN	high			XXX		
	low	XXX	XXX			
skin	high			XXX	XXX	
	low	XXX		XXX	XXX	
lung	high				XXX	XXX
	low	XXX	XXX		XXX	
penis	high				XXX	
	low	XXX			XXX	
eye	high			XXX	XXX	XXX
	low	XXX	XXX	XXX	XXX	

Rivard, Venselaar, Beaulieu, *Med Phys* 36, 2136-2153 (2009)

Multimodal Imaging: post-Op dosimetry

Imaging modality-
- CT only – commonly used
- US only – better prostate contour
- MRI only – still challenging
- CT & MRI – good, but expensive
- CT & US – take advantage from both
- US & C-arm – real time/dynamic

Post-Op plans on CT post-implantation and on US images at the start of the procedure.

| Difference	Mean (%)	σ (%)	p-value
$D90_{CT}-D90_{pre-US}$	6.4	21.6	0.1097
$D100_{CT}-D100_{pre-US}$	−3.75	19.33	0.3052
$V100_{CT}-V100_{pre-US}$	−0.17	9.01	0.9186
$V150_{CT}-V150_{pre-US}$	7.29	18.03	0.0379

US/TRUS   CT
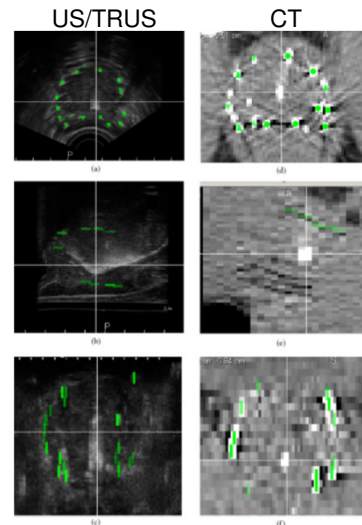
(a)–(c) A comparison of the visibility of implanted seeds on axial, sagittal and coronal views of a prostate implant on US images acquired using twister mode that was performed at the end of implantation procedure. (d)–(f) CT images acquired nearly 4 weeks post-implantation.
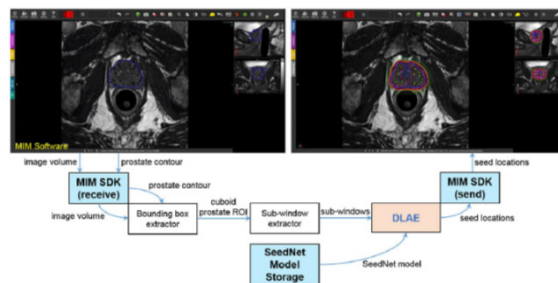
Ali, Spencer et al., Phys. Med. Biol. (2009) 54:5595–5611

Multimodal Imaging: post-Op dosimetry

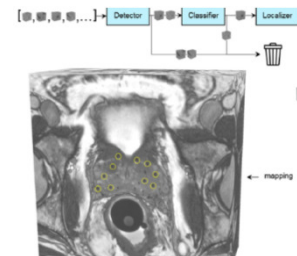**MRI only post-Op planning**
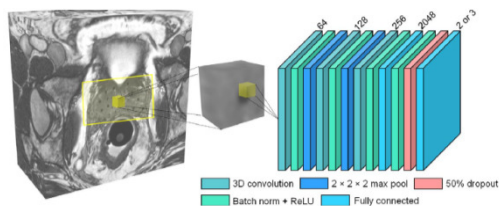
The SeedNet architecture. The windows were processed with 3D CNNs. Three separate CNNs, each with the same configuration of layers, were trained to perform seed detection, classification, and localization tasks.

First, each sub-window was passed to the detector to identify windows containing seeds. The seed sub-windows were then passed to a classifier to reject seed marker sub-windows that, owing to their similar shape and proximity to the seeds, were incorrectly classified as seed sub-windows. The seed sub-windows from the classifier were passed to the localizer to pinpoint the precise location of the seed. Finally, the seed sub-windows were mapped back to their locations within the original image stack.

Data-flow diagram demonstrating the integration of SeedNet into a clinical software package using DLAE.
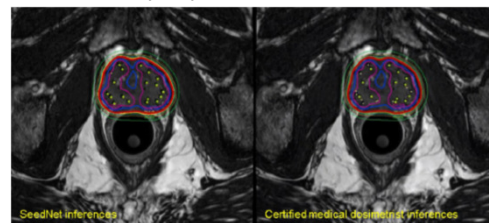
Example of SeedNet's (left) and a CMD's (right) seed location inferences and corresponding radiation dose distributions in MIM Software. The prostate contour was deactivated to allow for unobscured visualization of the isodose lines. The radioactive seeds are depicted as green circles.

Sander, Frank et al., Magn Reson Med. (2019) 81:3888-3900

Real-time Dynamic Dose Computation

- Used TRUS and C-arm fluoroscopy
- fluoroscopy-to-TRUS registration
- Seed segmentation: 1% false negative rate and 2% false positive
- Ability to detect cold spots
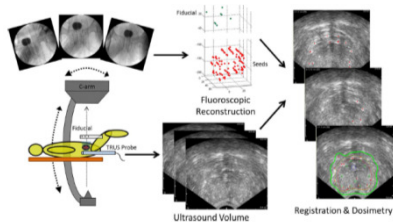
Workflow of our image-guidance system for dynamic dose calculation. At least three fluoroscopic images are taken of the implanted seeds and the fiducial above the patient's abdomen (the dark round object in the images is a Foley catheter balloon optionally filled with contrast to identify the bladder). An ultrasound volume of the seed-filled prostate is acquired. Both image sets are processed to calculate dose.
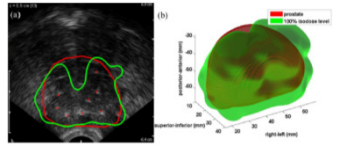

Intraoperative dosimetry result showing a cold spot. (a) TRUS image is overlaid with the prostate contour and the 100% isodose level (bright line) computed from the registered seed reconstruction (dots). (b) 3D rendering of the same prostate and 100% isodose level; cold spot is evident at the anterior base of the prostate.

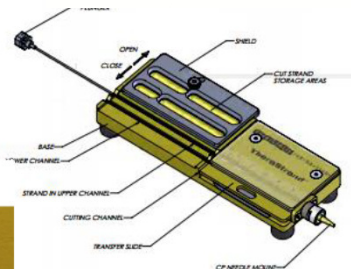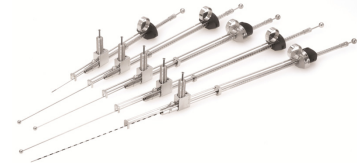| Patient	Reconstruction error (mm), mean ± Std		Registration error (mm), mean ± Std				Prostate dose metrics			
	Overall	x	y	z	Overall		D_{90} US/FL (%)	D_{90} MR/CT (%)	V_{100} US/FL (%)	V_{100} MR/CT (%)
1	0.8 ± 0.3	0.4 ± 0.5	0.4 ± 0.4	1.2 ± 0.9	1.6 ± 0.8		129	123	99.0	99.5
2	0.4 ± 0.4	0.3 ± 0.2	0.2 ± 0.3	0.7 ± 1.0	0.9 ± 0.9		125	115	94.8	95.1
3	0.3 ± 0.2	0.4 ± 0.4	0.9 ± 0.8	0.9 ± 0.9	1.6 ± 1.0		114	115	93.0	95.1
4	0.4 ± 0.2	0.3 ± 0.3	0.7 ± 0.3	0.8 ± 0.7	1.2 ± 0.6		153	130	98.9	98.0
5	0.6 ± 0.4	0.3 ± 0.3	0.5 ± 0.4	0.5 ± 0.3	0.9 ± 0.4		131	126	97.1	98.6
6	0.6 ± 0.5	0.6 ± 0.9	0.8 ± 0.7	0.7 ± 0.3	1.4 ± 0.9					
7	0.6 ± 0.3	0.3 ± 0.4	0.4 ± 0.3	0.9 ± 0.7	1.1 ± 0.7		132	100	98.3	90.1
8	0.5 ± 0.3	0.5 ± 0.4	0.5 ± 0.4	0.6 ± 0.3	1.1 ± 0.4		136	134	99.8	99.0
9	1.2 ± 1.3	0.4 ± 0.3	0.5 ± 0.4	0.9 ± 0.6	1.2 ± 0.4		125	118	97.4	97.6
10	0.5 ± 0.5	0.2 ± 0.2	0.5 ± 0.5	0.9 ± 0.7	1.2 ± 0.7		115	115	97.0	99.0
11	0.4 ± 0.3	0.4 ± 0.3	0.5 ± 0.5	1.1 ± 0.7	1.4 ± 0.6		123	125	94.3	98.5
12	0.4 ± 0.2	0.4 ± 0.4	0.5 ± 0.4	0.8 ± 0.6	1.2 ± 0.5		154	146	99.4	99.8
13	0.3 ± 0.2	0.4 ± 0.5	0.7 ± 0.6	0.8 ± 0.7	1.4 ± 0.5		131	118	99.3	97.3
14	0.3 ± 0.2	0.3 ± 0.3	0.5 ± 0.2	0.8 ± 0.7	1.1 ± 0.6		113	109	95.2	93.2
15	0.9 ± 0.6	0.2 ± 0.2	0.6 ± 0.5	1.0 ± 0.7	1.3 ± 0.6		108	106	93.2	93.8
16	0.3 ± 0.4	0.2 ± 0.2	0.4 ± 0.3	0.8 ± 0.7	1.1 ± 0.6		143	146	99.5	98.6
17	0.4 ± 0.4	0.2 ± 0.1	0.4 ± 0.3	0.9 ± 0.8	1.2 ± 0.7		140	151	98.9	99.6
18	0.5 ± 0.5	0.4 ± 0.5	0.7 ± 0.6	0.8 ± 0.5	1.4 ± 0.5		169	146	98.6	99.2
19	0.4 ± 0.3	0.2 ± 0.1	0.4 ± 0.3	0.5 ± 0.3	0.8 ± 0.3		130	132	97.8	98.7
20	0.4 ± 0.3	0.5 ± 0.5	0.2 ± 0.2	0.9 ± 0.5	1.2 ± 0.5		117	124	93.6	98.5
21	0.4 ± 0.3	0.3 ± 0.2	0.8 ± 0.6	1.0 ± 0.6	1.4 ± 0.6		137	124	99.3	97.6
22	0.2 ± 0.2	0.1 ± 0.1	0.7 ± 0.8	1.0 ± 0.5	1.3 ± 0.8		132	139	97.0	99.5
23	0.5 ± 0.7	0.3 ± 0.2	0.9 ± 0.5	0.8 ± 0.6	1.3 ± 0.7		165	144	96.8	99.3
24	0.4 ± 0.3	0.4 ± 0.4	0.5 ± 0.6	1.3 ± 1.0	1.7 ± 0.8		115	113	95.3	96.1
25	0.3 ± 0.7	0.4 ± 0.4	0.5 ± 0.4	1.4 ± 1.3	1.7 ± 1.2					
26	0.3 ± 0.2	0.2 ± 0.2	0.6 ± 0.6	0.9 ± 0.6	1.2 ± 0.5		114	110	96.8	96.9
27	0.3 ± 0.4	0.5 ± 0.4	0.6 ± 0.4	0.7 ± 0.5	1.1 ± 0.5		125	107	95.4	92.0
28	0.3 ± 0.2	0.1 ± 0.0	0.4 ± 0.3	0.9 ± 0.6	1.0 ± 0.6		127	118	98.5	95.3
29	0.5 ± 0.4	0.4 ± 0.4	0.5 ± 0.6	0.9 ± 0.8	1.2 ± 0.9		136	129	99.6	98.5
30	0.3 ± 0.2	0.5 ± 0.3	0.6 ± 0.6	1.0 ± 0.7	1.4 ± 0.6		124	106	96.1	93.9
31	0.5 ± 0.3	0.3 ± 0.4	0.4 ± 0.4	1.0 ± 1.1	1.3 ± 1.0					
32	0.3 ± 0.2	0.5 ± 0.6	0.4 ± 0.3	0.8 ± 0.7	1.2 ± 0.7		119	130	94.1	98.4
33	0.2 ± 0.2	0.6 ± 0.6	0.6 ± 0.4	1.2 ± 0.7	1.7 ± 0.7					
34	0.2 ± 0.2	0.4 ± 0.4	0.4 ± 0.4	0.5 ± 0.3	0.9 ± 0.3		125	123	96.4	94.9
35	0.3 ± 0.2	0.3 ± 0.2	0.4 ± 0.4	1.0 ± 0.7	1.3 ± 0.6		116	119	93.9	96.4
36	0.3 ± 0.2	0.3 ± 0.3	0.4 ± 0.3	0.5 ± 0.6	0.9 ± 0.5					
37	0.2 ± 0.2	0.6 ± 0.3	0.7 ± 0.6	0.8 ± 0.6	1.4 ± 0.5		120	124	94.6	96.9
Overall	0.4 ± 0.5	0.4 ± 0.4	0.5 ± 0.5	0.9 ± 0.7	1.3 ± 0.7					

Kuo, Dehghan et al., MedPhys (2014) 41(9):1-13

Treatment Delivery

1) Loose seeds stacked in cartridge – Mick Applicator
2) Pre-loaded needles
3) Seeds in a strand – preordered/cut or make in OR
4) Mechanized device – robotic systems

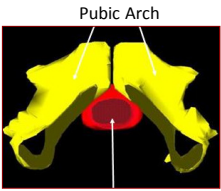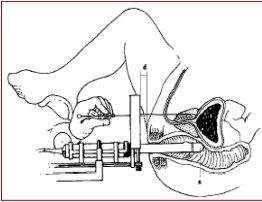Device to make strands
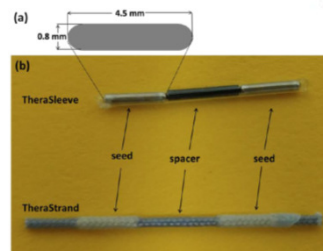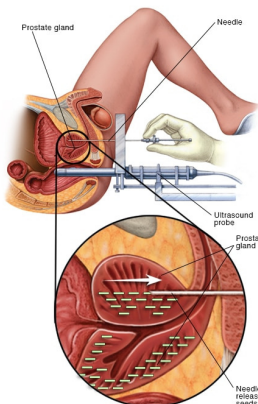
Seed strands: (a) seed dimension, (b) strands
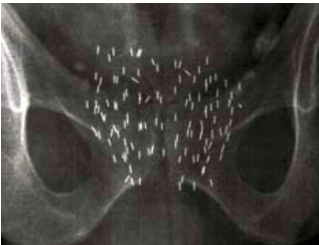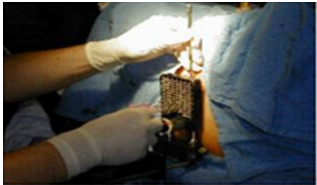
Conventional Prostate Seed Implant

Pubic Arch

Prostate

Fixed template

Needle angulation

Fatigue & exposure

- **Fixed template** – limited maneuverability
- **PAI** (pubic arch interference) – needle angulation difficult
- **Consistency, accuracy, efficiency** – techniques & human factors
- Clinicians' fatigue, commitment

Technical Challenges in Prostate Seed Implantation

- Edema – prostate volume increases, dose uncertainty, toxicities

- Needle placement – deflection from desired coordinates, difficulties in puncturing prostate capsule, prostate deformation deflection, i.e. challenge in immobilization

- Seed position – local movement, long distance migration (lungs, heart); position of delivered seeds can be significantly different from pre/intra-Op planned coordinates resulting in substantial deviation in dosimetric coverage

- Post-Op evaluation – challenging to delineate prostate in post-Op CT, several seeds may clamp together

11

Techniques for Prostate Immobilization

Hook needle   Regular needle

Methods for prostate stabilization during transperineal LDR brachytherapy

Tarun Podder[1], Jason Sherman[2], Deborah Rubens[3], Edward Messing[4], John Strang[5], Wan-Sing Ng[6] and Yan Yu[7]

[1] Department of Radiation Oncology, Jefferson Medical College, Thomas Jefferson University, Philadelphia, PA 19107, USA
[2] Department of Medical Physics, University of Buffalo, Buff
[3] Departments of Imaging Science and Surgery, University of USA
[4] Departments of Urology and Surgery, University of Rochest
[5] Departments of Imaging Science and Surgery, University of USA
[6] School of Mechanical and Aerospace Engineering, Nanyang Singapore 639798
[7] Department of Radiation Oncology, Jefferson Medical Colle Philadelphia, PA 19107, USA

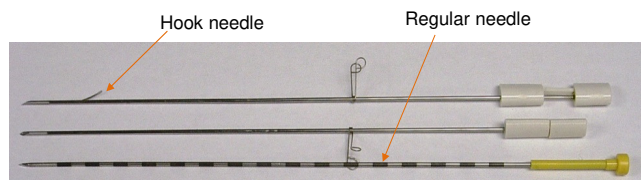**Table 7.** Overall prostate displacement results for all the configurations (*in vitro* experiment).

Needle	Needle configuration	Resultant displacement (mm)	Reduction in movement
No stabilization	–	15.4	–
18G Regular	Parallel (0°H0°V)	11.5	25.3%
18G Regular	20°H30°V	7.2	53.2%
18G Regular	30°H30°V	6.1	60.4%
18G Regular	30°H30°V crossed	5.6	63.6%
18G Hook	Parallel (0°H0°V)	6.5	57.8%
18G Hook	20°H30°V	6.3	59.1%
18G Hook	30°H30°V	5.7	63.0%

Rectilinear vs. Curvilinear Techniques for PSI
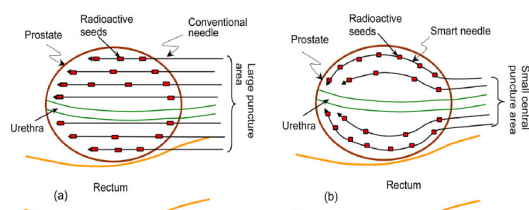
(a) Conventional rectilinear approach.

(b) Curvilinear conformal smart needle insertion.

Cumulative DVH

Conventional **rectilinear** implantation (**dotted** lines)
Proposed **curvilinear** implantation (**solid** lines)

CL in legend stands for "Curvilinear"

TABLE I. Comparison of proposed curvilinear approach and conventional rectilinear approach.

20 patient PSI cases

Parameter (n = 20)	Rectilinear method Average ± SD (range)	Curvilinear method Average ± SD (range)	Difference	p-value (two-tailed)
Total needle	19.2 ± 2.6 (14–23)	13.2 ± 1.4 (10–15)	−6.0 (−30.5%)	< 0.001
Total seed	62.5 ± 11.2 (43–85)	55.1 ± 10.4 (38–74)	−7.4 (−11.8%)	< 0.49
Total activity (mCi)	38.3 ± 6.3 (28.3–47.3)	33.8 ± 4.9 (25.3–40.3)	−4.5 (−11.8%)	< 0.37
Prostate (average = 41.3 cm³, range = 26.6–53.2 cm³):				
D₉₀ (Gy)	198.7 ± 9.9 (182.9–215.2)	183.3 ± 6.8 (176.3–194.5)	−15.4 (−7.8%)	< 0.04
V₁₀₀ (cm³)	99.98 ± 0.06 (99.8–100)	99.97 ± 0.06 (99.83–100)	−0.01 (−0.01%)	< 0.85
V₁₅₀ (cm³)	80.9 ± 6.8 (68.5–89.8)	65.7 ± 5.3 (57.8–75.9)	−15.2 (−18.8%)	< 0.01
V₂₀₀ (cm³)	43.7 ± 6.0 (32.7–53.4)	28.9 ± 3.3 (26.0–35.5)	−14.8 (−33.9%)	< 0.001
Urethra:				
D₁₀ (Gy)	209.9 ± 12.2 (186.2–228.7)	189.2 ± 8.1 (178.3–208.8)	−20.7 (−9.9%)	< 0.02
D₃₀ (Gy)	205.1 ± 10.4 (184.3–219.9)	184.3 ± 7.4 (172.5–200.2)	−20.8 (−10.1%)	< 0.01
Rectum:				
D₅ (Gy)	160.2 ± 15.9 (137.9–196.8)	130.5 ± 12.3 (111.0–151.1)	−29.7 (−18.5%)	< 0.03
V₁₀₀ (cm³)	0.93 ± 0.51 (0.19–2.0)	0.21 ± 0.17 (0.03–0.61)	−0.72 (−77.8%)	< 0.001

Podder, Dicker et al., MedPhys (2012) 39(4):1887-1892

Other Challenges

- Brachytherapy is underrated/underappreciated
- Shadowed by proton therapy and IMRT
- Decreasing expertise
- Increasing lack of BT training; needs to shorten and make it popular

Robotic BT devices can mitigate some of the above issues

Robot-assisted Brachytherapy
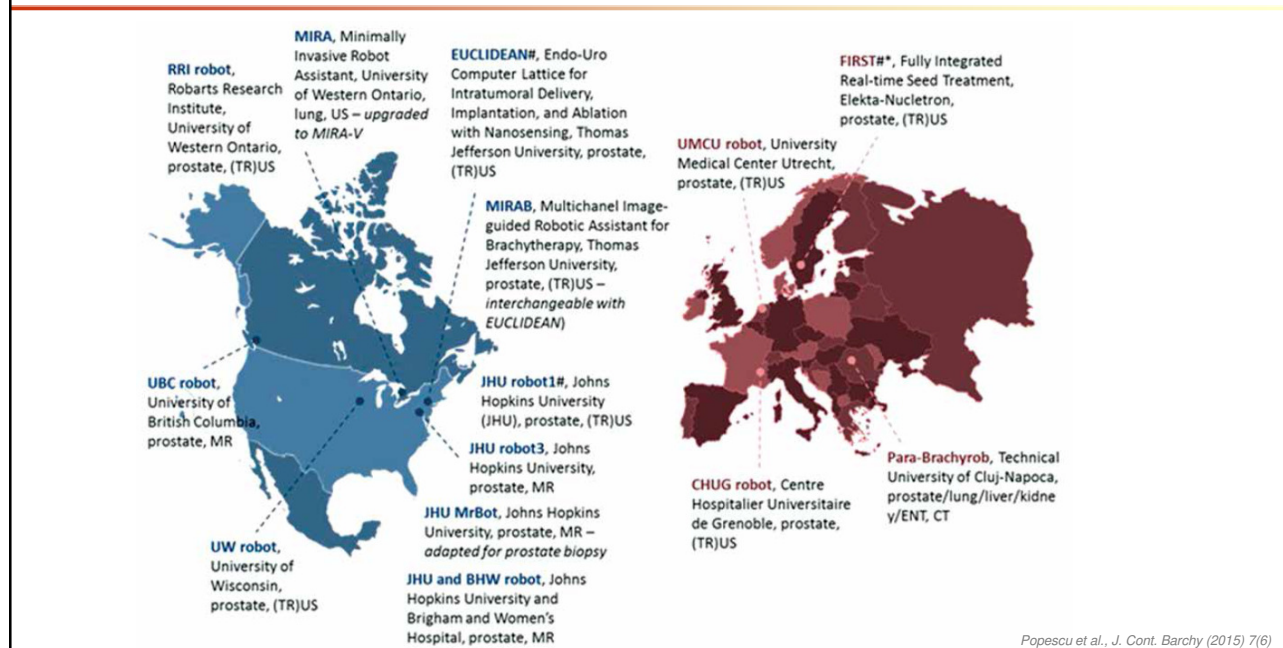
Main Objectives are to -

1) Improve accuracy of needle/catheter placement
2) Improve consistency of source placement/delivery
3) Improve avoidance of OARs
4) Improve dose optimization
5) Reduce the clinician's learning curve
6) Reduce clinician's fatigue
7) Reduce radiation exposure to clinical staff
8) Streamline the brachytherapy procedure

AAPM TG-192, MedPhys (2014) 41(10)

Robotic Systems for Brachytherapy

RRI robot, Robarts Research Institute, University of Western Ontario, prostate, (TR)US

MIRA, Minimally Invasive Robot Assistant, University of Western Ontario, lung, US – *upgraded to MIRA-V*

EUCLIDEAN#, Endo-Uro Computer Lattice for Intratumoral Delivery, Implantation, and Ablation with Nanosensing, Thomas Jefferson University, prostate, (TR)US

FIRST#*, Fully Integrated Real-time Seed Treatment, Elekta-Nucletron, prostate, (TR)US

UMCU robot, University Medical Center Utrecht, prostate, (TR)US

MIRAB, Multichanel Image-guided Robotic Assistant for Brachytherapy, Thomas Jefferson University, prostate, (TR)US – *interchangeable with EUCLIDEAN)*

UBC robot, University of British Columbia, prostate, MR

JHU robot1#, Johns Hopkins University (JHU), prostate, (TR)US

JHU robot3, Johns Hopkins University, prostate, MR

JHU MrBot, Johns Hopkins University, prostate, MR – *adapted for prostate biopsy*

JHU and BHW robot, Johns Hopkins University and Brigham and Women's Hospital, prostate, MR

UW robot, University of Wisconsin, prostate, (TR)US

CHUG robot, Centre Hospitalier Universitaire de Grenoble, prostate, (TR)US

Para-Brachyrob, Technical University of Cluj-Napoca, prostate/lung/liver/kidney/ENT, CT

Popescu et al., J. Cont. Barchy (2015) 7(6)

Available/developed Robotic Systems for Brachytherapy

1) Thomas Jefferson University, USA (2) – Podder, Yu
2) Johns Hopkins University, USA (4) – Fichtinger, Stoianovici, Song
3) University of Wisconsin, USA (1) – Thomadsen, *et al.*
4) University of British Colombia, Canada (1) – Salcudean, Spadinger
5) Robarts Research Institute, Canada (1) – Fenster, *et al.*
6) University of Western Ontario, Canada (1) – Patel, *et al.*
7) Elekta/Nucletron - SeedSelectron/FIRST, Netherlands (discontinued) – Elekta
8) Univ. Medical Center Utrecht, Netherlands (1) – Moerland, Lagerburg
9) Grenoble University Hospital, France (1) – Troccaz, Hungr
10) Univ. of California at San Diego/ Univ. of Iowa (1) – Watkins, Song
11) Univ. of Cluj-Napoca, Romania (1) – Galdău, Pîslă
12) Tianjin Univ, China (1) – Dou, Yang, *et al.*
13) CoBra (MRI guided) - *European project*

Total = 17 robotic systems

14

Summary of Brachy Robots

**Table 1: Summary of the currently available robotic brachytherapy systems.**   Total = 17 (2 are not listed here, shown later)

| Features	TRUS-based Robotic Prostate Brachytherapy Systems								MR-based Robotic Prostate Brachytherapy Systems				US-based Robotic Brachytherapy Systems for Other Organs		
	FIRST	EUCLIDIAN	MIRAB	UW robot	JHU-robot1 (1)	UBC	RRI	CHUG	UMCU	JHU-MrBot (2)	JHU-MR (3)	JHU-MR (4)	MIRA-V	PARA –BRACHYROB	DMBT
Institute/Lab	Elekta-Nucletron	TJU	TJU	UW	JHU	UBC	RRI	CHUG	UMCU	JHU	JHU	JHU	UWO	TUCN	UCSD
Year (approx…)	2001-2004	2005-2010	2007-2012	2005-2008	2002-2008	2007-2009	2005-2011	2007-2011	2006-2010	2003-2008	2005-2008	2007-2011	2005-2009	2013-2016	2011-2016
RIA Class	2	3	3	2	2	2	2	2	2	2	2	2	3	2	3
Brachy Class	II	III	III	II	II	II	II	II	II	III	II	II	II	II	II
Application	PSI	PSI	PSI/HDR	PSI/HDR	PSI	PSI	PSI	PSI	PSI/HDR	PSI	PSI	PSI	LSI (lung)	Seed Implantation	HDR (rectum/breast)
Imaging modality	U/S (auto & manual)	U/S (auto & manual)	U/S (auto & manual)	U/S (manual)	U/S (manual)	U/S (manual)	U/S (auto & manual)	U/S (auto & manual)	MRI	MRI	MRI	MRI	U/S		
Degrees-of-freedom (DOF)	2 DOF	5 DOF surgical, 2 DOF U/S, 6 DOF positioning, 3 DOF cart	5 DOF surgical, 2 DOF U/S, 6 DOF positioning, 3 DOF cart	6 DOF	4 DOF surgical	4 DOF surgical	U/S (auto & manual)	5 DOF	5 DOF	4 DOF	3 DOF	6 DOF	5 DOF	5 DOF	3 DOF (including HDR source movement)
Number of channel/ needle	Single	Single	16 needles	Single	Single	Single	Single	Single	Single	Single	Single	Single	Single	Single	8-16 channels
Needle insertion	Manual	Autonomous	Autonomous	Auto and /or Manual	Manual	Manual	Manual	Autonomous	Autonomous tapping	Autonomous			Manual	Autonomous	N/A
Needle rotation	No	Yes	Yes	Yes	No	No	Manual	Yes	No	No	No	No	No	No	N/A
Angled Insertion	No	Yes		Yes	Yes	Yes	Yes	Yes	Yes	No	Yes	Yes	Yes	Yes	N/A
Source delivery/ positioning	Autonomous	Autonomous	Autonomous	Manual (auto in research)	Manual	Manual	Manual	Manual	Manual	Autonomous	Manual	Manual	Manual	N/A	Autonomous
Needle/source withdraw	Autonomous	Autonomous	Autonomous	Auto and /or Manual	Manual	Manual	Manual	Manual	Manual	Autonomous	Manual	Manual	Autonomous	Autonomous	Autonomous
Physical template	Yes	Yes	Yes	No	No	No	No	No	No	No	No	No	No	No	No
Template/perineum area coverage	Conventional	62mm x 67mm	60mm x 60mm	250mm x 250mm	50mm x 50mm	150mm x 50mm	60mm x 60mm	105mm x 105mm	N/A	40mm x 40mm	N/A	50mm x 50mm	N/A	N/A	N/A
Depth movement	Conventional	312mm	240mm	250mm	120mm	150mm	70mm	N/A	150mm	40mm	N/A	120mm	N/A		45mm
TPS	Oncentra Seeds	In-house, FDA- IDE approved	In-house	N/A	FDA approved Interplant	N/A	In-house	N/A	N/A	N/A	N/A	none	N/A	N/A	N/A
Needle tip positioning accuracy in air	N/A	< 0.2 mm	< 0.2mm	N/A	N/A	<0.3mm	0.2mm	1.0mm	N/A	0.32mm	N/A	0.94mm	<0.5mm	N/A	N/A
Needle tip positioning accuracy in phantom	<0.5mm	<0.5mm	<0.5mm	N/A	1.04mm	N/A	0.9mm	1.0mm	N/A	<0.5mm	2.0mm	3.0mm	0.9mm	N/A	N/A
Accuracy in source/seed deposition	<1mm (tested)	<1mm (tested)	<1mm	<1mm	N/A	1.2mm	1.6mm	N/A	N/A	<1mm	N/A	N/A	N/A	N/A	1mm
Emergency stop	Yes	Yes	Yes	Yes	Yes	Yes	Yes	Yes	Yes	Yes	Yes	Yes	Yes	N/A	N/A
Provision for reverting to conventional mode	Yes	Yes	Yes				Yes		No					N/A	N/A
Force-torque sensor	No, but motor stops if too much force needed)	Yes	No	Yes	No	No	No	No	No	No	No	No	No	N/A	N/A
FDA, CE approval	Yes, also CE	IDE	No	No	No	No	No	No	No	No	No	No	No	No	No

Some of the Brachy Robots
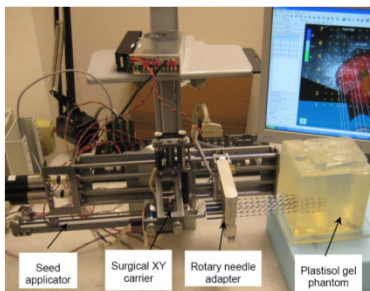

Stoianovici, Roach, *et al.* MITAT, 2010
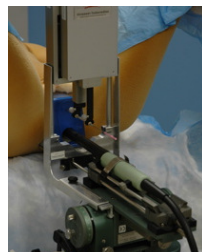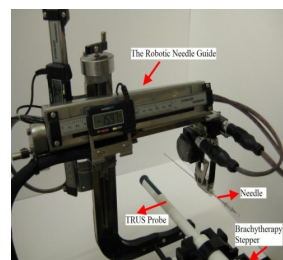
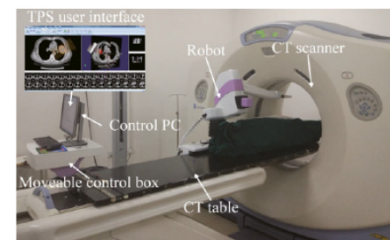Fichtinger *et al.* MedIA, 2008
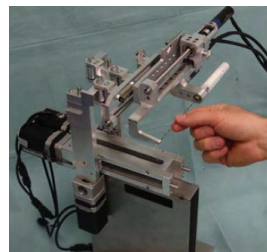
Hungr, *et al.* IEEE-EMBS, 2009

Yu, Podder *et al.* MICCAI 2006

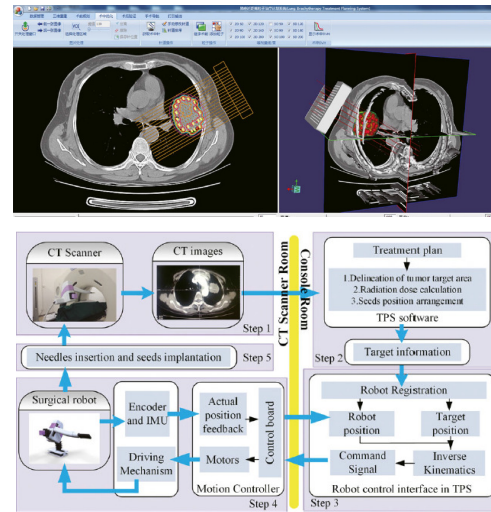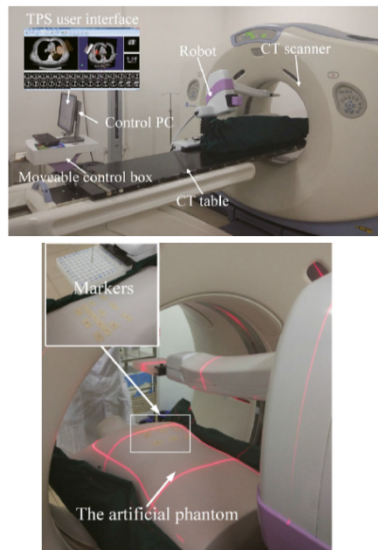Podder et al. IEEE-BIBE 2010

Salcudean et al. IEEE-ICRA 2010

Dou, *et al.* MedPhys 2017
(4DOF CT-guided for lung brachy)

CT-guided Robotic System for Lung Brachy

Robot-assisted seed implantation for lung cancer.
Used this system for treating over 34 NSCLC patients since 2015.

Dou, Yang et al., MedPhys (2017) 44(9)

coBra robotic system (MRI-guided)

- Multiple sensors (force/torque, optical range, radiation) – improve safety and reliability
- Automatic seed deposition – less burden for clinicians
- Needle rotation – reduces insertion force, improves targeting
- Needle angulation – a few puncture at the perineum, avoidance of PAI
- Cartridge with 100 seeds – less radiation exposure, saves time

https://youtu.be/3f41dV8EIT4
https://cobra-2seas.eu/
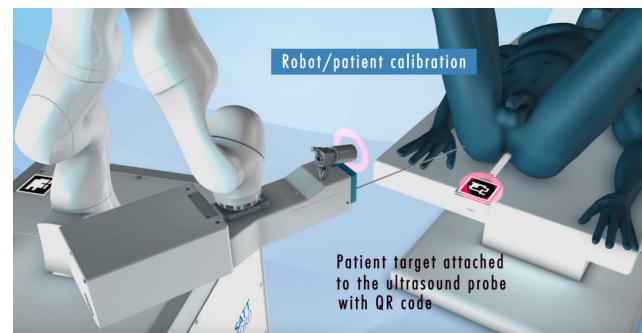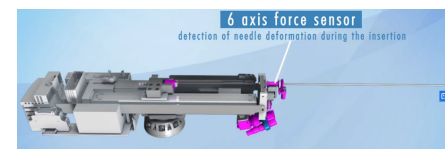
Future Directions

1) Use of multimodal imaging and mpMRI for cancer detection and diagnosis – radiomics, AI/ML, ANN/CNN etc.

2) Consider focal therapy – reduce toxicity, improve quality of life

3) Improve dosimetric computation – MC, MBDC, etc.

4) Improve delivery of Tx – target stabilization, accurate needle placement and seed deposition, real-time dynamic dose verification and adaptation

5) Training of new generation – physicians & physicists

6) Use mechanized/robotic systems – reduce clinician's burden, improve Tx consistency

7) Respect and follow the science

Summary

➢ Multimodal imaging is critical for PSI

➢ Radiomics, AI/ML may play important role

➢ Dose paining to DIL/mpMRI can reduce toxicity and may improve clinical outcome

➢ Mechanized/ robot-assisted Tx delivery can improve consistency & quality of implant and may reduce some burdens of the clinicians

Thank You!

Stay Safe!!

Any Question?